A Comparison Study of Deep CNN Architecture in Detecting of Pneumonia

First version

Al Mohidur Rahman Porag
Department of Computer Science and Engineering
Daffodil International University
Dhaka, Bangladesh
Porag15-3462@diu.edu.bd

Md. Mahedi Hasan
Researcher
Department of Computer Science and Engineering
Daffodil International University
Dhaka, Bangladesh
mh.cse9@gmail.com

Dr. Md Taimur Ahad
Associate Professor
Department of Computer Science and Engineering,
Daffodil International University
Dhaka, Bangladesh
taimur.cse0396.c@diu.edu.bd

***Abstract*— Pneumonia, a respiratory infection brought on by bacteria or viruses, affects a large number of people, especially in developing and impoverished countries where high levels of pollution, unclean living conditions, and overcrowding are frequently observed, along with insufficient medical infrastructure. Pleural effusion, a condition in which fluids fill the lung and complicate breathing, is brought on by pneumonia. Early detection of pneumonia is essential for ensuring curative care and boosting survival rates. The approach most usually used to diagnose pneumonia is chest X-ray imaging. The purpose of this work is to develop a method for the automatic diagnosis of bacterial and viral pneumonia in digital x-ray pictures. This article first presents the authors' technique, and then gives a comprehensive report on recent developments in the field of reliable diagnosis of pneumonia. In this study, here tuned a state-of-the-art deep convolutional neural network to classify plant diseases based on images and tested its performance. Deep learning architecture is compared empirically. VGG19, ResNet with 152v2, Resnext101, Seresnet152, Mobilenettv2, and DenseNets with 201 layers are among the architectures tested. Experiment data consists of two groups, sick and healthy X-ray pictures. To take appropriate action against plant diseases as soon as possible, rapid disease identification models are preferred. DenseNets has shown no overfitting or performance degradation in our experiments, and its accuracy tends to increase as the number of epochs increases. Further, DenseNets achieves state-of-the-art performance with a significantly a smaller number of parameters and within a reasonable computing time. This architecture outperforms the competition in terms of testing accuracy, scoring 95%. Each architecture was trained using Keras, using Theano as the backend.**

Keywords— Pneumonia; Chest X-ray images; Convolution Neural Network (CNN), Transfer Learning, Ensemble Model, Deep Learning.

I. INTRODUCTION

Acute pulmonary infection (pneumonia) is a condition in which the lungs become inflamed due to infection with bacteria, viruses, or fungi; this leads to a condition known as pleural effusion, in which the lungs become swollen with fluid. More than 15% of all deaths in children younger than 5 can be attributed to this cause. Countries with high rates of population growth, pollution, and poor sanitation have the highest rates of pneumonia, and these countries also have the fewest available medical resources to treat the disease. Therefore, preventing the disease from progressing to a deadly stage requires prompt diagnosis and treatment. In this research, we built a CAD system that correctly classifies chest X-rays using an ensemble of deep transfer learning models.

Deep learning is a crucial artificial intelligence tool for solving many complicated computer vision problems. Image categorization uses deep learning models, particularly convolutional neural networks (CNNs) problems. Such models work best with lots of data. Because professional clinicians must classify each image, obtaining such a large volume of labeled data for biomedical image classification tasks is expensive and time-consuming. Transfer learning circumvents this issue. This method applies network weights from a model trained on a large dataset to a small dataset problem. Biomedical image categorization often uses CNN models trained on ImageNet, which has over 14 million images. Data scientists have been drawn to the concept of utilizing Deep Convolutional Neural Network (D-CNN) in identifying, classifying, and segmenting brain tumors as a result of the visible benefits of Deep Convolutional Neural Network (D-CNN) in Medical Image Analysis. When it comes to segmenting the timorous region included inside a brain, D-CNN is a set of techniques that has the potential to produce better outcomes when compared to techniques that do not involve deep learning. The multilayered, hierarchical, and block structure of D-CNN allows for the extraction of low-, mid-, and high-level information from pictures of brain tumors. D-CNN shows an outstanding performance in solving the segmentation and classification issues that are based on time and effort consuming tasks like fractionalization of brain tumor cells in Medical Image scans. This is in contrast to the large amount of time and effort that is required for the segmentation process by doctors and radiologists due to the high quantity of data produced by scan centers.

Using the well-liked technique of ensemble learning, the judgments of various classifiers are combined to get the final prediction for a test sample. It is carried out to extract the discriminative information from each base classifier, producing more precise predictions as a result. Average probability, weighted average probability, and majority

voting are some of the ensemble techniques that have been utilized in research in the literature most frequently. Each constituent base learner is given equal priority by the average probability-based ensemble. But for a specific issue, one basic classifier might be better equipped to gather data than another. Therefore, weighting all of the base classifiers is a better technique. However, the importance of the weights given to each classifier is the most important component in ensuring the ensemble's improved performance. The majority of methods base this number on the outcomes of experiments. In this study, we developed a novel weight allocation method in which the best weights for three base CNN models—SeresNet152, ResNet152v2, and DenseNet-201, Vgg-19, and Resnext101—were determined using four evaluation metrics: precision, recall, f1-score, and area under the receiver operating characteristics (ROC) curve (AUC). For providing weights to the base learners in research in the literature, only classification accuracy was often taken into account [8], which may not be a sufficient metric, especially when the datasets are class imbalanced. Other indicators might offer more useful data for deciding how important the basic learner is.

II. LITERATURE REVIEW

This review of the relevant literature is structured in two main sections: the first discusses the concept of CNN variations, while the second focuses on CNN's application to the detection and segmentation of pneumonitis.

A. The Introduction Of Disease

A lung inflammation known as pneumonia primarily affects the tiny air sacs known as alveoli. Common symptoms include a combination of a dry or productive cough, chest pain, fever, and breathing difficulties. The disorder can range in severity. The most frequent germs that cause pneumonia are viruses and bacteria, although other microbes can also cause it. It can be challenging to pinpoint the virus at fault. The physical exam and symptoms are frequently used to make a diagnosis. Blood tests, sputum cultures, and chest X-rays can all help confirm the diagnosis. The location of the infection, such as community, hospital-, or healthcare-associated pneumonia, can be used to classify the illness.

Cystic fibrosis, chronic obstructive pulmonary disease (COPD), sickle cell disease, asthma, diabetes, heart failure, a history of smoking, a bad cough reflex (such as after a stroke), and a weakened immune system are among the risk factors for pneumonia. There are vaccines available to protect against specific types of pneumonia, including those brought on by the Streptococcus pneumoniae bacteria, linked to influenza, or linked to COVID-19. Other preventative strategies include not smoking, hand washing to avoid infection, and social seclusion. The underlying reason determines the course of treatment. Antibiotics are used to treat pneumonia that is thought to be caused by bacteria. The patient is typically hospitalized if the pneumonia is severe. If oxygen levels are low, oxygen therapy may be employed.

B. Original CNN Networks

In a convolutional neural network (CNN), the term "convolution" refers to the mathematical fusion of two functions to create a third function. When it occurs, two sets of data are combined. CNN contains a number of layers arranged in succession as opposed to an Artificial Neural Network (ANN), which only has one layer. CNNs use a convolutional layer (also known as a filter or kernel) to transform the input data into a feature map. An input layer, numerous convolutional layers, pooling layers, a fully connected layer, and eventually an output layer make up this layering system in detail. The remaining layers—aside from the input and output layers — are referred to as hidden layers.

CNN has built a model of the human brain using the mixture of these networks. CNN layers are organized so that simpler patterns (lines, curves, etc.) are detected initially and more complicated patterns (faces, objects, etc.) are detected afterwards. However, CNN has drawn a lot of interest in data science since it has demonstrated its ability to locate, segment, and identify objects in images. In this study, the term "original CNN architecture" refers to a CNN network and algorithm that are available on Keras or Github. In this study, the CNN algorithm is used exactly as its creators and programmers intended it to be, with no modifications to its processing units, parameterization and hyper-parameter optimization methodologies, design patterns, or layer connections. A well-known CNN network was frequently created and improved by several researchers and programmers over the course of numerous difficulties.

VGG19: A variant of VGG with 19 layers enables explicit and effective spatial information propagation between neurons in the same layer of a CNN (see figure 1). It is extremely effective in cases where objects have strong shapes. The main contribution is a thorough evaluation of networks of increasing depth using an architecture with very small (3×3) convolution filters but still captures left/right and up/down). There are also 1x1 convolution filters which act as a linear transformation of the input, which is followed by a ReLU unit. The convolution stride is fixed to 1 pixel so that the spatial resolution is preserved after convolution.

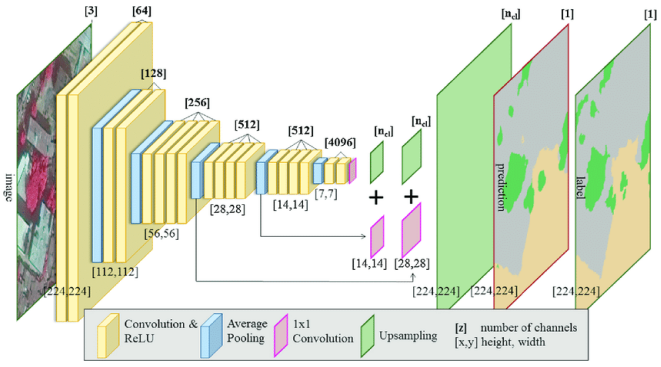

Figure 1: Schematic representation of VGG19 (source google)

ResNet152v2: The ResNet architecture (and its three realizations ResNet-50, ResNet-101, and ResNet-152) was introduced by Microsoft Research Asia in 2015 and achieved outstanding outcomes in the ImageNet and MS-COCO competitions. Residual connections, the central concept used in these models, are discovered to significantly increase gradient flow, enabling training of much deeper models with tens or even hundreds of layers. Through their distinct WordNet IDs, ImageNet classes are mapped to Wolfram Language Entities. This is particularly a problem in deep networks because the value of gradient can vanish, i.e. shrink to zero, when several chain rules applied consecutively. Skipping connections will help gradients flow backwards directly from end layers to initial layer filters, enabling CNN models to deepen with 152 layers. In the field of image recognition and localization tasks, ResNet has a strong performance that demonstrates the importance of many visual recognition task.

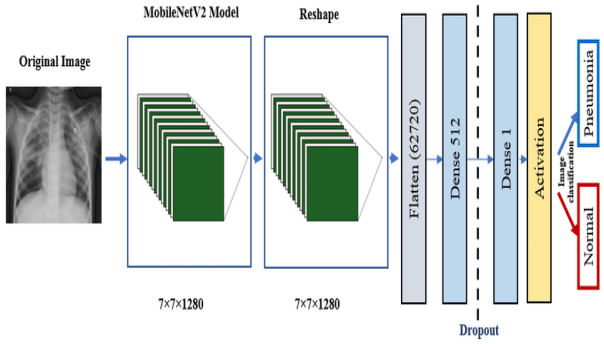

Figure 2: Schematic representation of ResNet152v2 (source google)

DenseNet201: By leveraging shorter connections between the layers, the DenseNet (Dense Convolutional Network) design aims to increase the depth of deep learning networks while also improving training efficiency. A convolutional neural network called DenseNet connects every layer to every other layer below it. For example, the first layer is connected to the second, third, fourth, and so on levels, and the second layer is connected to the third, fourth, fifth, and so on layers. In order to maximize information flow between network tiers, this is done. Each layer receives input from all the layers that came before it and transmits its own feature maps to all the layers that will follow it in order to maintain the feed-forward nature. Contrary to Resnets, it concatenates the features rather than combining them by summation. As a result, the "ith" layer contains I inputs and is made up of feature maps from all the convolutional blocks that came before it. All of the subsequent "I-i" layers receive its own feature map information. Instead of only 'I' connections as in conventional deep learning architectures, this adds '(I(I+1))/2' connections to the network. As a result, it needs fewer parameters than conventional convolutional neural networks because no unimportant feature maps need to be learned.

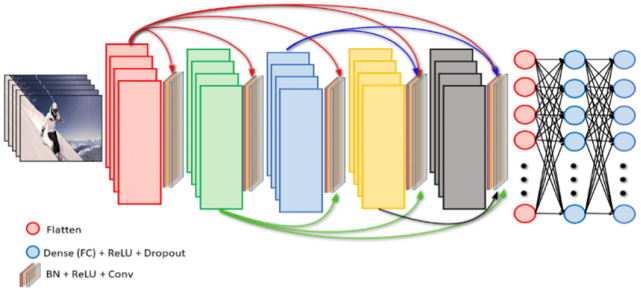

Figure 3: DenseNet201 Schematic Representation (source google)

MobileNetV2*:* It is an architecture for CNN that is designed to function effectively on mobile devices. It is predicated on an inverted residual structure, in which the connections for the residual elements are found between the bottleneck layers. In order to filter features and create a source of non-linearity, the intermediate expansion layer makes use of lightweight depth-wise (Dwise) convolutions. The initial fully convolutional layer in its architecture consists of 32 filters, and it is followed by 19 layers that are considered to be residual bottleneck layers. Figure 4 presents the MobileNetV2 network architecture for your perusal.

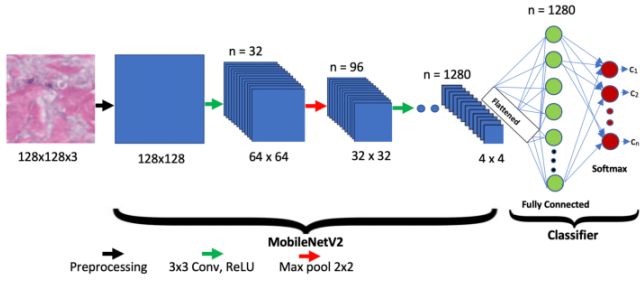

Figure 4: Schematic representation of MobileNetV2 (source google)

SeresNet152: The ResNet protocol is utilized as the foundation for this architecture. At the conclusion of the processing of each non-identity branch of the residual block, a block consisting of a squeeze and an excitation is applied. For a more in-depth analysis of the network's physical layout.

ResNeXt101: ResNeXt is a homogeneous neural network that cuts down on the number of hyperparameters that are necessary for a normal ResNet. This is made possible through the utilization of something called "cardinality," which is an additional dimension in addition to the width and depth of ResNet. The size of the set of transformations is determined by the property known as cardinality.
In this picture, the diagram on the left represents a traditional ResNet block, and the diagram on the right represents a ResNeXt block, which has a cardinality of 32.

The 32 iterations of the same alterations are carried out, and the final product is aggregated afterward.

Table 1. Comparison of CNN architectures applied in this study (M = Million)

Architecture Name	Year	Main contribution	Number of Parameters	No of layer	Reference
VGG	2014	- Homogenous topology - Uses small size kernels	138 M	19	Spatial Exploitation
ResNet	2016	- Residual learning - Identity mapping-based skip connections	25.6 M 1.7 M	152 110	(Kannappan et al. 2020)
Xception	2017	- Depth-wise convolution followed by point wise convolution	22.8 M	126	(Ruba et al. 2022)
ResNeXt	2017	- Cardinality - Homogeneous topology - Grouped convolution	68.1 M	29 - 101	(Mehta and Arbel 2018)
Squeeze & Excitation Networks	2017	- Models interdependencies between feature-maps	27.5 M	152	(Brunese et al. 2020)
DenseNet	2017	- Cross-layer information flow	25.6 M 25.6 M 15.3 M 15.3 M	190 190 250 250	(Brunese et al. 2020)

Apart from the solo CNN architectures, CNN has extended to transfer learning, ensemble technique, and region-based research. Following sections discuss these approaches of CNN.

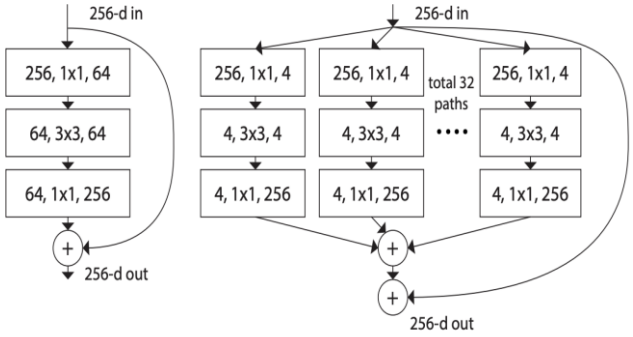

Figure 5: Schematic representation of ResNeXt101

C. *Transfer learning*

Transfer learning technique is a method that builds on the understanding from a training dataset used for training in a different activity or field. However, the final few layers of the trained network can be discarded and retrained with new layers for the target task. The first few layers of this deep learning process are trained to describe the properties of the task. It describes a scenario in which what has been discovered in one context is used to enhance optimization in another. We investigate the CNN architecture's topology in an effort to identify a model that will enable Transfer Learning to classify images. Although with limited processing power and time, testing and altering the network topology (i.e., parameters) as well as dataset characteristics might assist identify the factors that affect classification performance.

As a function of the model performance, training a deep learning model with a limited data set is frequently undesirable. Transfer learning is the process of initializing a model with weights from another model that has been trained on a bigger, unrelated dataset. Only when the segmentation problem is more difficult and the target training data is less are significant improvements shown.

Training a deep learning model with a small data set is often undesirable as a function of the model performance. Transfer learning is the process of pre-initializing a model using weights obtained by training a different model on a larger, different, dataset. Large improvements are observed only when the segmentation task is more challenging and the target training data is smaller.

D. *Ensemble technique*

Ensemble Learning is one of the DL technologies which combines multiple primary learners through a fusion strategy to improve the overall generalization performance. Ensemble learning is one of the deep learning technologies, that combines multiple primary learners through a fusion strategy to improve the overall generalization performance. Ensemble learning has attracted wide attention due to its easily understandable structure and promising classification of generate a marker at a suspicious region in a mammogram.

Ensemble learning is a technique that incorporates multiple models for final decision-making. The ultimate goal of an ensemble is that by combining multiple models, the errors of a single model can be corrected (compensated) by other models, thereby making the overall result (prediction and classification) of the ensemble better than any single participating model.

E. *Deep CNN/ Machine learning on Pneumonia*

As was previously said, CNNs have gained popularity as a result of their enhanced picture classification capabilities. The network's convolutional layers and filters aid in the extraction of an image's spatial and temporal information. The weight-sharing method used by the layers aids in minimizing computational effort.

In terms of architecture, CNNs are just feedforward artificial neural networks (ANNs) with two restrictions: to preserve spatial structure, neurons in the same filter can only be connected to small patches of the image; additionally, their weights must be shared to minimize the number of

parameters in the model. Three components make up a CNN: a convolution layer for learning features, a max-pooling (subsampling) layer for downsampling the picture and reducing its dimensionality, which reduces computational cost, and a fully connected layer for giving the network classification skills.

An ensemble of global and local-attention based convolutional neural networks for COVID-19 diagnosis on chest X-ray images by A. Afifi et al.[1] on (2021).

The deep-learning approach uses an ensemble of CNN models to detect global and local disease characteristics in CXR lung pictures. In a multi-label classification framework with COVID-19, pneumonia, and control classes, an ensemble of DenseNet161 models with global and local attention-based features achieves 91.2% balanced accuracy, 92.4% precision, and 91.9% F1-score. A detailed statistical investigation found the DenseNet161 ensembles statistically significant from all other models.[1]

Epidemiology of community-acquired pneumonia in adults: A population- based study by J. Almirall *et al.*[2] *(2000).*

In this prospective study, the authors assessed the incidence, aetiology, and outcome of patients with community-acquired pneumonia in the general population. From December 1993 to November 1995, a study was performed in a mixed residential-industrial urban population of the 'Maresme' region in Barcelona, Spain. All subjects ≥14 yrs of age (annual average population size 74,368 inhabitants) with clinically suspected community- acquired pneumonia were registered. [2]

Artificial intelligence on COVID-19 pneumonia detection using chest xray images on (2021) by L. R. Baltazar *et al.*[3]

AI can screen chest x-ray (CXR) pictures for COVID-19 pneumonia, according to recent studies. However, medical and technical concerns about datasets, study methods, and AI algorithm vulnerability and robustness have arisen. Optimized five deep learning architectures and executed development strategies by changing data distribution to statistically evaluate research designs. In a two-class detection situation, InceptionV3 had the greatest Sn, Sp, and PPV of 96% for differentiating pneumonia from normal CXR. Compared to four-class detection, three-class detection yielded 91-96% Sn, 94-98% Sp, and 90-96% PPV. In the three-class detection situation, InceptionV3 performs best with 96% accuracy, F1-score, and g-mean. InceptionV3 has the highest Sn, Sp, PPV, and AUC for COVID-19 pneumonia identification. It had 0.98 AUC for COVID-19 pneumonia and 0.99 for other classes.[3]

Community-acquired pneumonia in adults: Guidelines for management on 1998 by J. G. Bartlett et al.[4]

The Infectious Diseases Society of America's recommendations are included in this paper. Only immunocompetent adult patients with community-acquired pneumonia are covered by the guidelines. diagnostic research The report offers suggestions for diagnosing individuals with probable pneumonia, emphasizing the critical importance of chest radiography in determining the existence of a parenchymal infiltration.[4]

ChxCapsNet: Deep capsule network with transfer learning for evaluating pneumonia in paediatric chest radiographs on (2022) by J. D. Bodapati et al.[5]

In this study, a deep neural network model was created to quickly assess juvenile pneumonia in chest radiograph pictures. Our comparison analyses show that the suggested model, which combines an InceptionV3 Convolution base with final Capsule layers, outperforms numerous other models by obtaining an accuracy of 94.84%. In comparison to manual chest radiography examination, the suggested model performs better on a variety of performance metrics like recall and accuracy. It is also well suited to real-time pediatric pneumonia diagnosis.[5]

A novel transfer learning based approach for pneumonia detection in chest X-ray images on (2020) by V. Chouhan *et al.*[6]

This study simplifies pneumonia detection for professionals and beginners. We propose a transfer learning-based pneumonia detection deep learning framework. Different neural network models pretrained on ImageNet extract picture features, which are fed into a classifier for prediction. We tested five models. We then suggested an ensemble model that included outputs from all pretrained models, which outperformed individual models and reached state-of-the-art pneumonia recognition. Our ensemble model had 96.4% accuracy and 99.62% recall on unseen Guangzhou Women and Children's Medical Center data.[6]

Molecular Diagnosis of a Novel Coronavirus (2019-nCoV) Causing an Outbreak of Pneumonia on (2020) by D. K. W. Chu *et al.*[7]

Positive and negative controls assessed these assays. Two 2019-nCoV-infected patients had respiratory specimens tested. RESULTS: These experiments had a dynamic range of at least seven orders of magnitude (2x10-4-2000 TCID50/reaction) using SARS coronavirus-infected cell RNA as a positive control. These tests detected < 10 copies per reaction using DNA plasmids as positive standards. Assays were negative for all negative controls. Two 2019-nCoV patients tested positive.[7]

Detection of Pneumonia with a Novel CNN-based Approach on (2021) by E. ERDEM et al.[8]

Pre-trained and suggested deep learning models were compared. Deep learning structure accuracy is 88.62%. The new deep neural network approximated VGG16 (88.78%) and VGG19 (88.30%) accuracy scores. Our model has a higher recall value (97.43%) and F1-Score (91.45%) than VGG16 (91.22%) and VGG19 (91.19%).[8]

Diagnostic and prognostic prediction models in ventilator-associated pneumonia: Systematic review and meta-analysis of prediction modelling studies on (2022) by T. Frondelius et al.[9]

Expert systems have not improved ventilator-associated pneumonia diagnosis (VAP). This comprehensive literature review summarized state-of-the-art VAP prediction models based on exhaled breath, patient reports, and demographic and clinical variables. Methods: Representative multidisciplinary databases were examined for diagnostic and prognostic prediction models. To find publications without predictive research in their titles or abstracts, a long list of validated search phrases was included. Two authors independently selected research, while three writers extracted data using predetermined criteria and data extraction forms.[9]

Mortality and severity evaluation by routine pneumonia prediction models among Japanese patients with (2009) pandemic influenza A (H1N1) pneumonia on by Y. Fujikura *et al.*[10]

surveyed Japanese adult influenza pneumonia patients nationwide. 2491 hospital respiratory medicine physicians received questionnaires. Using invasive positive pressure ventilation (IPPV) as an indication, PSI, CURB-65, and A-DROP assessed pneumonia severity and outcome (age, dehydration, respiration, disorientation, and blood pressure). Results: 25 deaths (7.8%) and 43 IPPV (13.4%) were found in 320 influenza pneumonia patients.[10]

Predicting post-stroke pneumonia using deep neural network approaches on (2019) by Y. Ge *et al.*[11]

The attention-augmented GRU model performed best with an AUC of 0.928 for pneumonia prediction within 7 days and 0.905 for pneumonia prediction within 14 days. This strategy beat machine learning-based and previously reported pneumonia risk score models. We also examined prediction performance using other evaluation criteria by setting the sensitivity to 0.90, since pneumonia prediction after stroke requires a high sensitivity to prevent it at a low cost (i.e., increasing the nursing level). The attention-augmented GRU had the highest specificity of 0.85, PPV of 0.32, and NPV of 0.99 for pneumonia within 7 days.[11]

Hybrid quantum-classical convolutional neural network model for COVID-19 prediction using chest X-ray images on (2022) by E. H. Houssein et al.[12]

This research presents an HQ-CNN model that uses random quantum circuits to detect COVID-19 patients in chest X-ray pictures. HQ-CNN was evaluated using 5445 chest X-ray pictures, including 1350 COVID-19, 1350 normal, 1345 viral pneumonia, and 1400 bacterial pneumonia. The first trial showed 98.6% accuracy and 99% recall for the suggested HQ-CNN model (COVID-19 and normal cases). The second experiment yielded 98.2% accuracy and 99.5% recall (COVID-19 and viral pneumonia cases). The third dataset yielded 98% accuracy and 98.8% recall (COVID-19 and bacterial pneumonia cases). On the multiclass dataset, it had 88.2% accuracy and 88.6% recall.[12]

Learning distinctive filters for COVID-19 detection from chest X-ray using shuffled residual CNN on (2021) by R. Karthik et al.[13]

The suggested work displays the salient X-ray locations that most significantly impacted CNN's prediction result. As far as we are aware, this is the first attempt in deep learning to develop customized filters within a single neural layer for recognizing particular pneumonia classes. Experimental findings show that the proposed study has a great deal of potential to improve the COVID-19 testing procedures now in use. On the COVID-19 X-ray set, it earns an F1-score of 97.20% and an accuracy of 99.80%.[13]

Pneumonia detection in chest X-ray images using an ensemble of deep learning models on 9 September, (2021) by R. Kundu et al.[14]

This work established a computer-aided pneumonia detection system using chest X-ray pictures. Deep transfer learning and an ensemble of three convolutional neural network models—GoogLeNet, ResNet-18, and DenseNet-121—were used to handle data scarcity. A unique weighted average ensemble strategy was used to award base learners weights. The weight vector is formed by fusing the scores of four conventional assessment metrics: precision, recall, f1-score, and area under the curve. Studies in the literature often set the weight vector empirically, which is error-prone. A five-fold cross-validation strategy was used to evaluate the suggested approach on two publically available pneumonia X-ray datasets from Kermany et al. and RSNA. On the Kermany and RSNA datasets, the technique had accuracy rates of 98.81% and 86.85% and sensitivity rates of 98.80% and 87.02%.[14]

Detection of Chlamydia pneumoniae in aortic lesions of atherosclerosis by immunocytochemical stain on (1993) by C. C. Kuo et al.[15]

Immunocytochemical analysis showed C pneumoniae antigens in aortic atheromas in autopsy individuals from retrospective aortic atherosclerosis investigations at the University of Washington. 34–58-year-old patients. Immunoperoxidase staining with Chlamydia-specific monoclonal antibodies revealed C pneumoniae antigens in one of four fatty streaks and six of 17 fibrous plaques. Four control aorta tissues were negative. Same patient had two positive plaques. Double-label immunocytochemical labeling with Chlamydia- and tissue type-specific monoclonal antibodies showed antigens in the cytoplasm of atheromatous lesion macrophages and smooth muscle cells. This study revealed a greater role for C pneumoniae pathogens in arterial atherosclerotic plaques.[15]

Nomogram for pneumonia prediction among children and young people with cerebral palsy: A population-based cohort study on (2020), by T. J. Kuo et al.[16]

This retrospective nationwide population-based cohort research tracked CYP with newly diagnosed severe CP before 18 years old from January 1, 1997, to December 31, 2013. Severe pneumonia requiring hospitalization was the main outcome. Severe pneumonia demographics and comorbidities were determined using logistic regression. A scoring system was created using integer points to identify children at high risk for serious pneumonia. Results 2,135 (33.59%) of 6,356 newly diagnosed severe CYP had severe pneumonia. Multivariable logistic regression revealed seven independent predicted factors: age <3 years, male sex, and comorbidities of pressure ulcer, gastric reflux, asthma, seizures, and prenatal problems.[16]

Multi-task contrastive learning for automatic CT and X-ray diagnosis of COVID-19 on (2021) by J. Li *et al.*[17]

COVID-19 diagnosis is the key task. First, each image is augmented to facilitate local aggregation by contrastive loss (Poisson noise, rotation, etc.). Then, the model is tuned to embed representations of the same picture similar and other images dissimilar in latent space. CMT-CNN can predict transformation-invariantly and preserve data spread-outness. The seemingly simple auxiliary job enhances generalization. We use free datasets and hospital data to create CT (4,758 samples) and X-ray (5,821 samples) datasets for experiments. Contrastive learning (plugins) improves deep learning model accuracy on CT (5.49%-6.45%) and X-ray (0.96%-2.42%) without annotations. Codes are online.[17]

Study of community acquired pneumonia aetiology (SCAPA) in adults admitted to hospital: Implications for management guidelines on 2001 by W. S. Lim *et al.*[18]

Results - 267 of 309 CAP patients met study criteria; 135 (50.6%) were men and the mean (SD) age was 65.4 (19.6) years. Aetiological agents were found in 199 (75%) patients: Streptococcus pneumoniae 129 (48%), influenza A virus 50 (19%), Chlamydia pneumoniae 35 (13%), Haemophilus influenzae 20 (7%), Mycoplasma pneumoniae 9 (3%), Legionella pneumophilia 9 (3%), other Chlamydia spp 7 (2%), Moraxella catarrhalis 5 (2%), Coxiella burnetii 2 (0.7%), others 8 (3%). Atypical infections were less common in 75-year-olds than younger patients (16% v 27%; OR 0.5, 95% CI 0.3 to 0.9). 30-day mortality was 14.9%. Four "core" unfavorable traits can predict mortality. Atypical pathogens killed three of 60 patients (5%). Conclusion: S pneumoniae is the most essential pathogen to cover with first antibiotic therapy in people of all ages hospitalized with CAP. Younger patients have more atypical pathogens. All severe pneumonia and younger non-severe infection patients should be covered.[18]

Identification of antibiotic resistance and virulence-encoding factors in Klebsiella pneumoniae by Raman spectroscopy and deep learning on (2022) by J. Lu *et al.*[19]

The MICs of 15 common antimicrobials on K. pneumoniae strains were determined. The InVia Reflex confocal Raman microscope collected 7,455 spectra for deep learning and ML algorithm analysis. Independent data estimated predictor quality. The CNN model simplified Raman spectroscopy classification and identified K. pneumoniae with high resistance and virulence more accurately than the SVM and LR models. We found that Raman spectroscopy may provide accurate and sensible treatment regimens for bacterial infections within hours by back-testing the Raman-CNN platform on 71 K. pneumoniae strains. More importantly, this strategy could cut healthcare costs and antibiotic usage, minimizing antimicrobial resistance and increasing patient outcomes.[19]

CovXNet: A multi-dilation convolutional neural network for automatic COVID-19 and other pneumonia detection from chest X-ray images with transferable multi-receptive feature optimization on (2020) byT. Mahmud et al.[20]

Due to test kit shortages, COVID-19 has made speedy diagnostic testing difficult. COVID-19 causes pneumonia, which must be identified immediately. This research proposes deep learning-aided automatic COVID-19 and pneumonia identification using a minimal number of chest X-rays. CovXNet, a deep convolutional neural network (CNN)-based architecture, extracts diverse information from chest X-rays using depthwise convolution with variable dilation rates. predictions, stacking is used. Finally, a gradient-based discriminative localization is used to identify aberrant X-ray pictures of distinct pneumonia kinds. Extensive experiments utilizing two datasets show excellent detection performance with 97.4% for COVID/Normal, 96.9% for COVID/Viral, 94.7% for COVID/Bacterial, and 90.2% for multiclass COVID/normal/Viral/Bacterial pneumonias.[20]

Infection with Chlamydia pneumoniae accelerates the development of atherosclerosis and treatment with azithromycin prevents it in a rabbit model on (1998) by J. B. Muhlestein *et al.*[21]

Background: Serological studies and plaque antigen detection have linked atherosclerosis to Chlamydia pneumoniae infection. We tested an animal model for causality. Methods and Results—30 New Zealanders White rabbits received three intranasal C pneumoniae (n=20) or saline (n=10) inoculations at 3-week intervals and were fed chow with 0.25% cholesterol. Infected and control rabbits were randomized to receive azithromycin or no treatment following the final inoculation. Three months after the final inoculation, rabbits were euthanized and thoracic aorta sections were blindly examined microscopically for maximal intimal thickness (MIT), percentage of luminal circumference involvement (PLCI), and plaque area index (PAI) of atherosclerosis. Immunofluorescence measured vascular chlamydial antigen. MIT differed among treatment groups (P=.009), with infected rabbits (0.55 mm; SE=0.15 mm) having a higher MIT than uninfected controls (0.16 mm; SE=0.06 mm) and infected rabbits receiving antibiotics (0.20 mm; SE=0.03 mm) (both P<.025), but not compared to control rabbits. Groups with a similar pattern differed in PLCI (P<.1) and PAI (P<.01). 2 untreated, 3 treated, and 0 controls had chlamydial antigen. Conclusions—Intranasal C

pneumoniae infection promotes intimal thickening in rabbits fed modes fly cholesterol-enriched diet. Weekly azithromycin prevents rapid intimal thickening following infection exposure. These findings enhance the causal relationship between C pneumoniae and atherosclerosis and should encourage animal and human studies, including clinical antibiotic trials.[21]

Lung X-Ray Image Enhancement to Identify Pneumonia with CNN on (2021) by N. Nafiiyah et al.[22]

High-contrast chest x-rays have varied intensities. For accurate diagnosis, chest X-rays need contrast stretching. The image intensity histogram can improve contrast. Chest X-rays detect pneumonia. Computers can diagnose pneumonia from chest x-rays. Pneumonia diagnosis by computer demands a trustworthy algorithm. Convolutional Neural Network, a trustworthy algorithm. This study investigated whether contrast-improved chest X-rays helped diagnose pneumonia. Pneumonia diagnosis using a Convolutional Neural Network. 8 CNN architectural models trained the CLAHE corrected chest X-ray. The training results of the eight CNN architectural models have loss function values of 0.0057, 0.028, 0.0964, 0.0446, 0.0473, 0.0573, 0.0979, 0.1407. Pneumonia diagnostic tests in the eight CNN architectural models yielded 79.65%, 79.01%, 80.29%, 76.92%, 82.53%, 80.45%, 79.81%, and 78.04%. The CNN 35 Layers architecture model using a grayscale 224x224 input image has the highest accuracy of 82.53%.[22]

A novel method for multivariant pneumonia classification based on hybrid CNN-PCA based feature extraction using extreme learning machine with CXR images on 2021M. Nahiduzzaman *et al.* [23]

Pneumonia identification and treatment are crucial during COVID19. Pneumonia diagnosis relies on CXR image analysis. This requires a skilled radiologist. CXR pictures are fuzzy, making diagnosis difficult and time-consuming even for experienced radiographers. Human judgment can sometimes lead to misidentification. Thus, a reliable, automated system is crucial. Deep learning (DL) is applied everywhere in this age of cutting-edge technology. Several pneumonia diagnosis procedures are inaccurate. This paper proposes a pneumonia detection technique using extreme learning machine (ELM) on Kaggle CXR pictures (Pneumonia). Extreme learning machine (ELM) classification, ELM with hybrid convolutional neural network-principal component analysis (CNN-PCA)-based feature extraction, and CNN-PCA-ELM with contrast-enhanced CXR pictures have been explored (CLAHE). The third model yields the most optimistic result. Multiclass pneumonia categorization yields 98% recall and 98.32% accuracy. Binary categorization has 100% recall and 99.83% accuracy. The proposed method outperforms previous methods. The outcome was compared using accuracy, precision, recall, etc.[23]

Siderophore production as a biomarker for Klebsiella pneumoniae strains that cause sepsis: A pilot study on (2021) by H. Namikawa *et al.*[24]

Background/purpose: Klebsiella pneumoniae bacteremia-induced sepsis has a significant death rate and many virulence factors. Here reviewed the medical records of 76 K. pneumoniae bacteremia patients from January 2012 to July 2017. 25 patients had sepsis, 51 did not. Background, antimicrobials, and prognosis were assessed. K. pneumoniae's mucoviscosity, capsular polysaccharide, and siderophores were examined. Results: Age and gender were similar between groups. Multivariable analysis showed that siderophore production level ($p < 0.01$) independently predicted K. pneumoniae bacteremia-induced sepsis. The best siderophore cut-off point to predict sepsis was 9.6 mm (sensitivity, 86%; specificity, 76%; AUC, 0.81). Conclusion: Siderophore synthesis independently predicted K. pneumoniae bacteremia-induced sepsis. Sepsis prediction was best at 9.6 mm siderophore production. Careful management of K. pneumoniae bacteremia-induced sepsis with high siderophore production improves outcomes.[24]

Transfer learning with deep Convolutional Neural Network (CNN) for pneumonia detection using chest X-ray on (2020) by T. Rahman *et al* .[25]

The paper uses digital x-rays to automatically detect bacterial and viral pneumonia. It describes pneumonia detection breakthroughs and the authors' technique. Transfer learning employed AlexNet, ResNet18, DenseNet201, and SqueezeNet, four pre-trained deep CNNs. 5247 bacterial, viral, and normal chest X-rays were preprocessed and trained for transfer learning-based categorization. This study classified pneumonia as normal, bacterial, or viral. Normal, bacterial, and viral pneumonia pictures had 98%, 95%, and 93.3% classification accuracy, respectively.[25]

A Prediction Model for Pediatric Radiographic Pneumonia on (2022) by S. Ramgopal et al.[26]

We conducted a single-center prospective analysis of lower respiratory infection patients aged 3 months to 18 years who had a CXR for CAP suspicion. We created a comprehensive model using penalized multivariable logistic regression and a parsimonious reduced model using bootstrapped backward selection models. We tested model performance at various expected risk thresholds. 253 (22.2%) of 1142 patients had radiographic CAP. CAP was strongly linked with age, longer fever duration, tachypnea, and localized reduced breath sounds in multivariable analysis. Rhinorrhea and wheezing harmed CAP. The bootstrapped reduced model kept age, fever duration, and decreased breath sounds. Reduced model receiver operating characteristic area was 0.80 (95% confidence interval: 0.77-0.84). 13 (5.7%) of 229 children with a projected risk <4% showed radiographic CAP (sensitivity of 94.9% at 4% risk threshold). 140 (61.1%) of 229 children with a predicted risk >39% had CAP (specificity of 90% at 39% risk threshold). Conclusion: Age, fever duration, and reduced breath sounds predict

radiographic CAP well. This model may aid CAP CXR and antibiotic selection after external validation.[26]

Clinical Performance of The call Score for the Prediction of Admission to ICU and Death in Hospitalized Patients with Covid-19 Pneumonia in a Reference Hospital in Peru on (2022) by R. P.- Rodriguez *et al.* [27]

Analytical cross-sectional observational study. We included "Dos de Mayo" National Hospital COVID-19 pneumonia patients. Rapid or molecular-diagnosed patients over 18 were included. Medical histories with gaps or bacterial or fungal pneumonia were eliminated. Medical records provided data. Mortality and ICU admission were key outcomes. Each patient's Call Score (4–13 points) was divided into three risk groups. Qualitative and quantitative variables were summarized. For the optimal cut-off point, the model curve area and operational characteristics (sensitivity, specificity) were computed. Results: Call Score predicted death with an area under the curve of 0.59 (IC95%: 0.3 to 0.07), p = 0.43. At 5.5, sensitivity was 87% and specificity was 65%. The area under the curve for ICU admission was 0.67 (95%CI: 0.3 to 0.07), p = 0.43; the 5.5 cut-off point had 82% sensitivity and 51% specificity.[27]

Surfactant protein D: a predictor for severity of community-acquired pneumonia in children on (2022) by N. Y. Saleh et al.[28]
Menoufia University Hospital's PICU and wards conducted a prospective cohort study. We recruited 112 children with uncomplicated pneumonia and 68 with severe pneumonia from wards and PICUs (PICU admitted). The WHO classification and mortality predicting scores, the Pediatric Respiratory Severity Score (PRESS) and the Predisposition, Insult, Response, and Organ dysfunction modified Score, were used to assess pneumonia severity in the two groups (PIROm). Admission measured SP-D. Results: Simple pneumonia patients had lower SP-D than severe pneumonia patients (P < 0.001). WHO, PRESS, and PIROm found increased SP-D in severe pneumonia children (P = 0.001). Mechanically ventilated children had greater SP-D. Receiver operating characteristic curve study for SP-D indicated an area under the curve of 0.741 (P value < 0.001), with 85.3% sensitivity and 44.6% specificity.[28]

On the detection of covid-19 from chest x-ray images using cnn-based transfer learning on (2020) by M. Shorfuzzaman et al.[29]
Menoufia University Hospital's PICU and wards conducted a prospective cohort study. We recruited 112 children with uncomplicated pneumonia and 68 with severe pneumonia from wards and PICUs (PICU admitted). The WHO classification and mortality predicting scores, the Pediatric Respiratory Severity Score (PRESS) and the Predisposition, Insult, Response, and Organ dysfunction modified Score, were used to assess pneumonia severity in the two groups (PIROm). Admission measured SP-D. Results: Simple pneumonia patients had lower SP-D than severe pneumonia patients (P < 0.001). WHO, PRESS, and PIROm found increased SP-D in severe pneumonia children (P = 0.001). Mechanically ventilated children had greater SP-D. Receiver operating characteristic curve study for SP-D indicated an area under the curve of 0.741 (P value < 0.001), with 85.3% sensitivity and 44.6% specificity.[29]

Efficient DNN Ensemble for Pneumonia Detection in Chest X-ray Images on (2021) by V. S. Suryaa et al.[30]
The World Health Organization (WHO) research states that severe pneumonia is the most typical diagnosis for severe COVID-19. Chest X-rays are the most popular way to diagnose pneumonia, but they take a lot of time and expertise to perform. In order to classify the images in this study and determine whether or not a person has pneumonia, feature extractors from pre-trained Convolutional Neural Networks (CNN) on chest x-ray images are utilized. With reference to their predictions on the photos, the various pre-trained Convolutional Neural Networks are evaluated using a variety of parameters. Pre-trained neural network outcomes were studied, and an ensemble model that combines the predictions of the best pre-trained models to outperform individual models was proposed.[30]

Detection and segmentation of lesion areas in chest CT scans for the prediction of COVID-19 on by A. Ter-Sarkisov et al.[31]
We contrast the models used in this paper to identify and classify Ground Glass Opacity and Consolidation in chest CT data. These lesion regions are frequently linked to both COVID-19 and common pneumonia. By combining the masks for these lesions into one, removing the mask for Consolidation, and using both masks individually, we train a Mask R-CNN model to segment these areas with excellent accuracy. Utilizing the MS COCO criterion for instance segmentation, the best model obtains a mean average precision of 44.68% across all accuracy thresholds. With only a small portion of the training data, the COVID-CT-Mask-Net classification model, which learns to distinguish between the presence of COVID-19, common pneumonia, and control, achieves the 93.88% COVID-19 sensitivity, 95.64% overall accuracy, 95.06% common pneumonia sensitivity, and 96.91% true negative rate on the COVIDx-CT test split (21192 CT scans). We also investigate the impact of overlapping item predictions' Non-Maximum Suppression on segmentation and classification precision.[31]

Predicting the 14-day hospital readmission of patients with pneumonia using artificial neural networks (Ann) on (2021) by S. F. Tey *et al.*[32]
This study developed a prediction algorithm to identify pneumonia patients with 14-day UPRA early. We collected 2016–2018 data from three Taiwanese hospitals on patients with pneumonia as the primary disease (ICD-10:J12*-J18*). 21,892 UPRA instances (1208 (6%)). To test model accuracy, ANN and CNN models were compared using the training (n = 15,324; 70%) and test (n = 6568; 30%) sets. An app predicts and classifies UPRA. We found that I the 17 feature variables extracted in this study provided a high area under the receiver operating characteristic curve of 0.75 using the ANN model, (ii) the ANN had a better AUC (0.73) than the CNN (0.50), and (iii) a ready-to-use app for UHA prediction was constructed.[32]

Significance of the modified nutric score for predicting clinical outcomes in patients with severe community-acquired pneumonia on (2022) by C. C. Tseng et al.[33] Clinical variables, the mNUTRIC score, and pneumonia prediction rules were reported. After discharge, mortality and treatment results were examined. The mNUTRIC score was compared to clinical prediction guidelines in 815 SCAP patients using the receiver operating characteristic (ROC) curve approach and multivariate logistic regression analysis. The mNU-TRIC score predicted clinical outcomes well and had the largest area under the ROC curve value. Clinical outcome prediction cut-off was 5.5. The mNUTRIC score independently predicted both clinical outcomes in SCAP patients by multivariate logistic regression analysis.[33]

III. EXPERIMENT DESCRIPTION

Using the Keras library, the experiments for this study were carried out on Google CoLab. For dealing with machine learning techniques on Python, TensorFlow, one of the best deep learning libraries, was employed. Each model was created by Google and made accessible through the Google Collaboratory framework after being trained in the cloud using a Tesla graphics processing unit (GPU). For research purposes, the Collaboratory framework offers up to 16GB of random-access memory (RAM) and roughly 360GB of GPU in the cloud.

In this study, the pneumonia detection architectures used were the original Vgg19, ResNet152v2, SeResNext101, ResNeXt101, DenseNet201, and MobileNetv2Using the Keras library, the experiments for this study were carried out on Google CoLab. For dealing with machine learning techniques on Python, TensorFlow, one of the best deep learning libraries, was employed. Each model was created by Google and made accessible through the Google Collaboratory framework after being trained in the cloud using a Tesla graphics processing unit (GPU). For research purposes, the Collaboratory framework offers up to 16GB of random-access memory (RAM) and roughly 360GB of GPU in the cloud.

One architecture was chosen from each category. There is overlap, though, as ResNet is classified as belonging to the depth, width, and malti-path categories. Other architecture (Inception from a depth-based and Densnet from a multi-path-based) was chosen in this circumstance.

A. Datasets

The dataset is divided into the following 3 folders: train, test, and val. Each image category (Pneumonia/Normal) has its own subfolder within the dataset. There are 2 categories (Pneumonia/Normal) and 5,863 X-Ray images in JPEG format. From retrospective cohorts of children patients aged one to five at the Guangzhou Women and Children's Medical Center in Guangzhou, chest X-ray images (anterior posterior) were chosen. All chest X-ray imaging was done as part of the regular clinical treatment provided to patient. All chest radiographs were initially checked for quality control before being removed from the study of the chest x-ray pictures. Before the diagnosis for the photos could be used to train the AI system, they were graded by two experienced doctors.

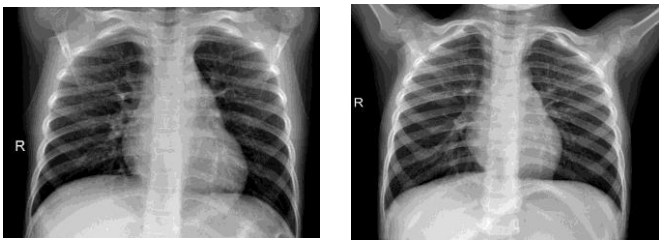

A. Normal

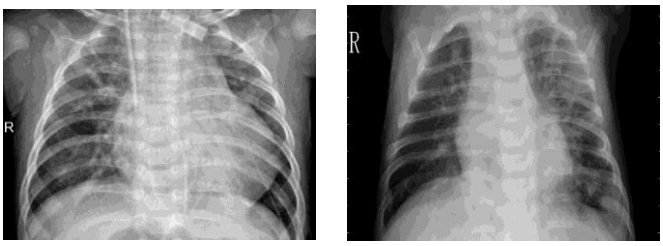

B. Pneumonia

Figure 6: Some Raw Image of Datasets

The evaluation set was additionally examined by a third specialist in order to account for any grading inaccuracies. Here the dataset link_ Chest X-Ray Images (Pneumonia) | Kaggle

Table 2. Images Used in the Train, Test and Validation Sets

	Normal	**Pneumonia**
Raw Dataset	1583	4265

B. Process of Experiments

The collecting of data from the X-ray images is the first step in the suggested structure. Data augmentation solutions are occasionally used to address the issue of constrained data since deep neural networks need additional data for training and increased performance. The following description of the experiment's working procedure:

Image Acquisition

The Pneumonia Image Database provided the data utilized to assess the model's performance. We successfully acquired images from the targeted websites for use in this step. Images in the dataset were manually checked to ensure they had a white background. Images with colored backgrounds are placed on a white background.

Image Augmentation

In this step, we are using image augmentation techniques to improve the image. Image augmentation is a technique that allows expanding an existing dataset by modifying it to generate additional new data while still keeping the original dataset's label information intact. The goal is to increase the variation in the data set while ensuring that new data are useful and do not simply add to the size of the data set. Using a larger data set can improve the generalization of a model, making it more resilient to unknown data. Additionally, using a machine learning model on this data can result in increased accuracy.

We used data augmentation methods to achieve the goals in the training data. However, color enhancement, such as brightness, contrast, and saturation, as well as position enhancement, by way of scaling, cropping, flipping, and revolution, was used. The technique of data enhancement also included random rotations from -15 to 15 degrees, rotations of 90 degrees by accident, accidental distortion, bending, vertical reversal, horizontal reversal, skate, and luminous intensity conversion. In this approach, 10 enhanced images were created from each original image. The selection of a subset of transformations helps to enhance a heterogeneous image.

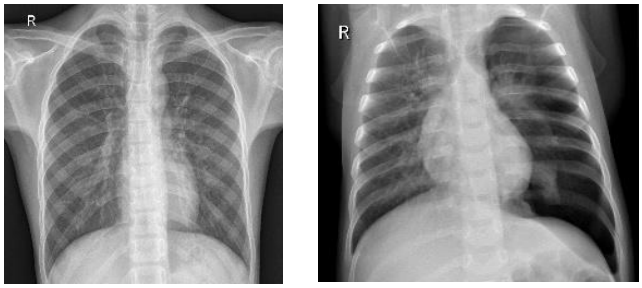

Figure 7: Augmented Image

Training

During this stage, a CNN learner model is built. A model was trained based on the given dataset and then assessed for classification accuracy using the architectures SeresNet152, MobileNetv2, ResNet152v2, ResNeXt100, Vgg19 and DenseNet201. All of the representations were trained with Early Stopping callbacks for 36 epochs (iterations) (patience = 10 iterations). The number of epochs without improvement after which training will be terminated is called patience. Stochastic Gradient Descent (SGD) with momentum and RMSProp are combined in an Adam optimizer (Root Mean Squared Propagation, or RMSProp, is a postponement of gradient parentage and the AdaGrad version of gradient descent that uses a decaying average of partial gradients in the adaptation of the step extent for each parameter were used for faster convergence with the parameters like learning rate was set at αα = 0.0001, β1β1 = 0.9, β2β2 = 0.999 and ϵ=1×10−7ϵ=1×10−7. For all three representations, a similar optimizer was used, and the models were then kept as.h5 files. Model training takes -45 seconds (s) per epoch (iterations) for MobileNet and 35 seconds (s) per epoch for DenseNet201 and Inceptionv3.

Because the dataset used in this experiment did not have any severe imbalances, the standard deviation was used as a model performance parameter in this study. Because this work deals with multi-class sorting, categorical cross-entropy was chosen as a loss task for all CNN architectures. The activation function employed in all transitional layers of the CNN architectures used in this study was relu, while the last layer's activation function was softmax. The following are the hyperparameters that were used: The dropout rate was 0.3, the learning rate was 0.0001, the batch size was 17, and there were 36 epochs. The model weights were updated using an adaptive moment estimation (Adam) optimizer. Before the resizing, all of the photographs were shrunk to the default image size for each architecture.

Classification

Neural networks (SerensNet152, MobileNetv2, VGG19, ResNet152v2, ResNeXt100 and DenseNet201) was used to detect cell illnesses automatically in this step. Because of its well-known technique as an effective classifier for many real-world applications, the neural network was chosen as a classification tool. Following the training model, a model for detecting blood cancer cells was created based on the highest probability of rate, and images of blood cells were sorted into distinct disease classes using a softmax output layer.

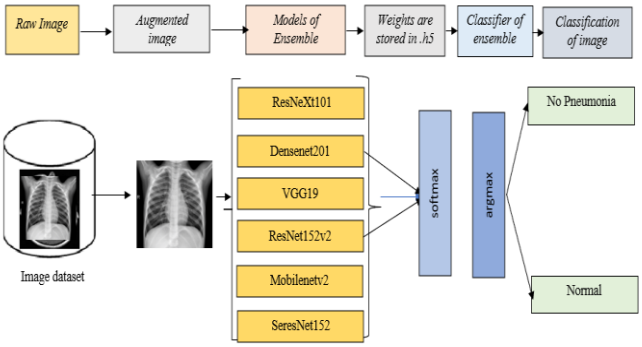

Figure 8: Process of Experiments.

Results

The findings are discussed in this section, followed by comparisons and discussions. The experiments' findings are divided into three sections: original individual network architectures, transfer learning, and ensemble techniques. All of the constraints are specified using trial and error approach, with the best set of parameter settings being reported.

Evaluation criteria

Several machine learning classification model performance measures are used to assess how well those CNN base algorithms perform in a given context. Accuracy (AC),

precision, recall, F1-score, and confusion matrix are among the performance metrics considered (CM). True positive (TP), true negative (TN), false positive (FP), and false-negative (FN) variables are also included in these metrics (FN). The following metrics are used to determine the criteria used to estimate the comparison's performance:

Accuracy

This metric takes into consideration the overall quantity of lessons correctly expected through the skilled version out of all feasible lessons. The ratio of efficaciously categorized images to the overall quantity of samples is described as accuracy.

$$\text{Accuracy} = \frac{TP+TN}{TP+TN+FP+FN}$$

Precision

This metric calculates the number of true positives among all positive cases. In the case of leukemia, the model can correctly identify those patients who have leukemia. When FP is more important than FN, precision is a useful metric. The following equation mathematically defines it:

$$\text{Precision} = \frac{TP}{TP + FP}$$

Recall

The recall metric measures how well the model highlights leukemia disease patients based on all relevant data. When FN triumphs over FP, recall becomes a useful metric. The following equation is used to calculate it:

$$\text{Recall} = \frac{TP}{TP + FN}$$

F-1 Score

The F1 score is an additional measure of classification accuracy that accounts for precision and recall. Because the F1-score is a harmonic mean of Precision and Recall, it is a synthesis of these two metrics. When Precision equals Recall, it is at its peak. By combining recall and precision values, this metric assesses the model's overall efficiency.

$$F-1\ \text{Score} = 2 * \frac{\text{Precision} * \text{Recall}}{\text{Precision} + \text{Recall}}$$

The training loss quantifies how well a model fits training data, whereas the validation loss quantifies how well a model fits new data. At its most basic, a loss characteristic quantifies how "good" or "bad" a given predictor is or classifies the entered facts in a dataset. The higher the category at modeling the connection among entering facts and output targets, the lower the loss. There is, however, a limit to how closely we can model the training data before our model loses its generalizability.

A confusion matrix (CM) is a type of table format that allows the performance of an algorithm to be evaluated. Important predictive analytics such as recall, specificity, accuracy, and precision are visualized using CM. Confusion matrices are beneficial because they allow for direct comparisons of values such as TP, FP, TN, and FN. Finally, the number of times the desired class inside the detailed dataset is known as a support. Imbalanced support inside the education facts might also additionally imply structural weaknesses inside the stated ratings of the classifier, indicating the need for stratified sampling or rebalancing. Based on the research questions, the sections that follow answer the research questions of this study.

IV. RESELT OF EXPERIMENT 1: ORIGINAL CNN

The performances of the six original individual CNN networks SecrensNet152, MobileNetV2, VGG19, ResNet152v2, ResNeXt100 and DenseNet201 are presented in this section. The models' classification performance is first presented. Following that, the overall measures for those models are discussed. gathering, in addition to descriptors, potential causes, and areas for improvement of results.

Table 3: Accuracy for Classification of Individual CNN Networks in Detecting Pneumonia (Original CNN Networks)

Architecture	**Training Accuracy**	**Model Accuracy**
VGG19	91.03%	92%
ResNet152v2	94.01%	94%
MobileNetv2	91.85%	92%
ResNeXt101	89.78%	90%
DenseNet201	94.34%	95%
SecrensNet152	90.49%	90%

The accuracy of the SecrensNet152, MobileNetV2, VGG19, ResNet152v2, ResNeXt101 and DenseNet201 is shown in Table 3. The ResNet152v2 models had the highest accuracy of 94%, while the SecrensNet152 and ResNeXt101 model had the lowest accuracy of 90%.

Table 4. Precision, Recall, F1-Score, and Support (n) result of original CNN networks (based on the number of images, n= numbers)

VGG19				
	Precision	**Recall**	**F1-Score**	**Support**
Normal	0.97	0.97	0.97	1353
Pneumonia	0.78	0.76	0.77	183
Accuracy			0.95	1536
Macro Avg	0.87	0.86	0.87	1536
Weighted Avg	0.94	0.95	0.95	1536

ResNet152v2				
	Precision	**Recall**	**F1-Score**	**Support**
Normal	0.96	0.98	0.97	1355
Pneumonia	0.80	0.66	0.72	181
Accuracy			0.94	1536
Macro Avg	0.88	0.82	0.85	1536
Weighted Avg	0.94	0.94	0.94	1536
MobileNetv2				
	Precision	**Recall**	**F1-Score**	**Support**
Normal	0.94	0.97	0.96	1397
Pneumonia	0.70	0.57	0.63	187
Accuracy			0.92	1584
Macro Avg	0.82	0.77	0.79	1584
Weighted Avg	0.91	0.92	0.92	1536
ResNeXt101				
	Precision	**Recall**	**F1-Score**	**Support**
Normal	0.93	0.96	0.94	1356
Pneumonia	0.59	0.47	0.52	180
Accuracy			0.90	1536
Macro Avg	0.76	0.71	0.73	1536
Weighted Avg	0.89	0.90	0.89	1536
DenseNet201				
	Precision	**Recall**	**F1-Score**	**Support**
Normal	0.97	0.76	0.97	1353
Pneumonia	0.78	0.95	0.77	183
Accuracy			0.86	1536
Macro Avg	0.87	0.95	0.87	1536
Weighted Avg	0.94	0.76	0.95	1536
SecrensNet152				
	Precision	**Recall**	**F1-Score**	**Support**
Normal	0.92	0.97	0.95	pp1352
Pneumonia	0.66	0.40	0.50	184
Accuracy			0.90	1536
Macro Avg	0.79	0.69	0.72	1536
Weighted Avg	0.89	0.90	0.89	1536

Table 4 shows the Precision, Recall, F1-score, and Support obtained by is shown in Table 3. The VGG19, DenseNet-201, and MobileNetv2 1 models for each class. When the precision values for each on the test dataset are considered, the VGG19, DenseNet-201, and MobileNetv2 architectures provide the best performance. According to the above table, the VGG19, DenseNet-201, SecrensNet152, and MobileNetv2 models correctly classified detecting. The ResNeXt100 performed poorly, with the lowest identification.

Training and Validation Accuracy and loss of Original CNN Networks:

Depicts the training and validation accuracy of the original model where the number of epochs is represented on the x-axis, and the accuracy and loss percentages are represented on the y-axis. The training and validation data are appropriately separated in the figure, and there is no over-fitting

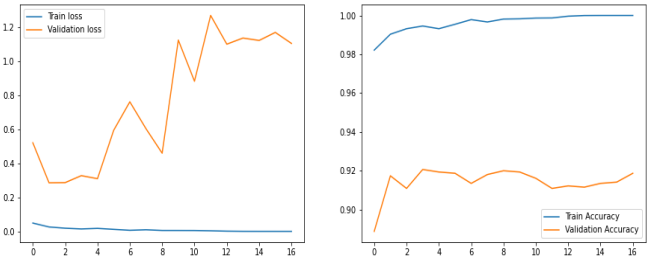

Figure 9: Training and validation accuracy and loss over the epochs (VGG Original CNN Networks).

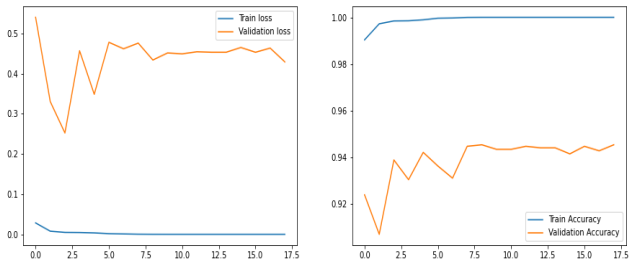

Figure 10: Training and validation accuracy and loss over the epochs (ResNet152v2 Original CNN Networks).

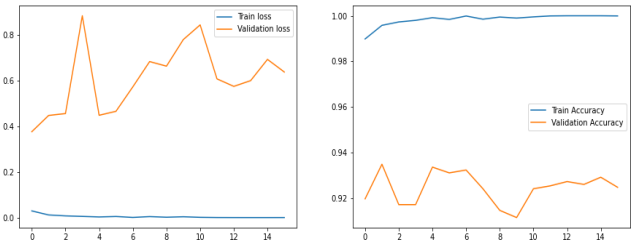

Figure 11: Training and validation accuracy and loss over the epochs (MobileNetv2 Original CNN Networks).

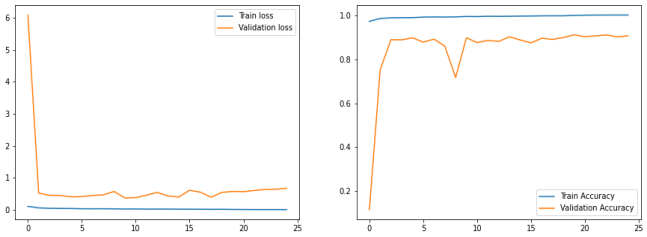

Figure 12: Training and validation accuracy and loss over the epochs (ResNeXt101 Original CNN Networks).

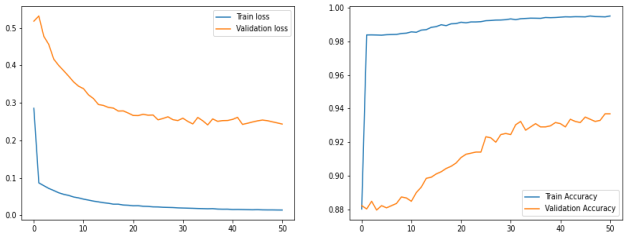

Figure 13: Training and validation accuracy and loss over the epochs (DenseNet201 Original CNN Networks).

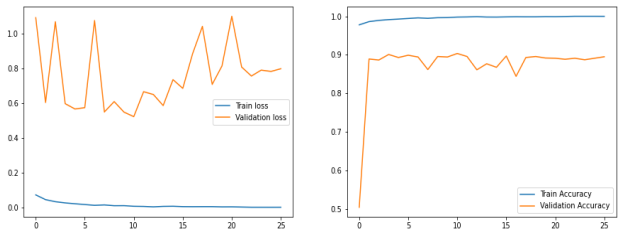

Figure 14: Training and validation accuracy and loss over the epochs (SecrensNet152 Original CNN Networks).

Confusion Matrix after Original:

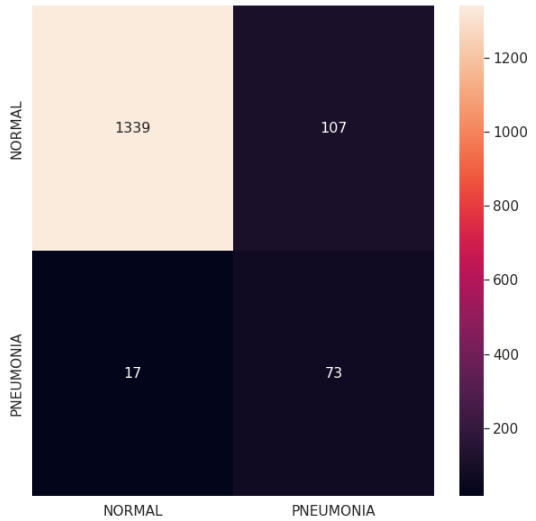

Figure 15: CM after Original Vgg19

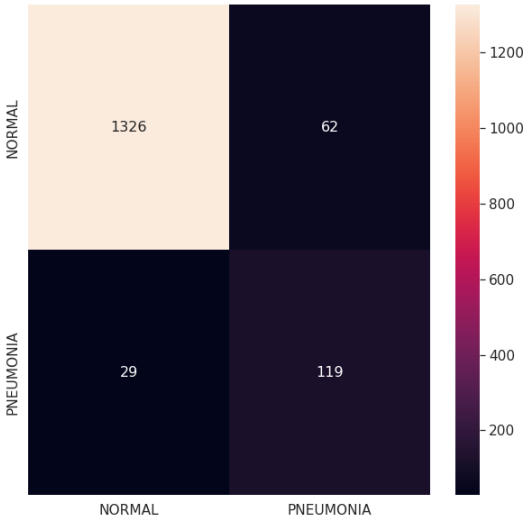

Figure 16: CM after Original ResNet152v2

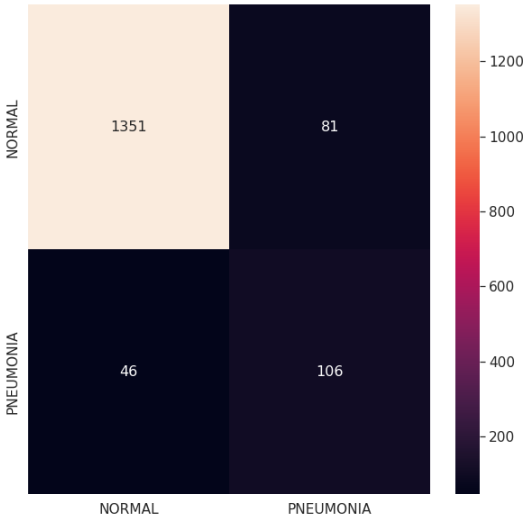

Figure 17: CM after Original MobileNetv2

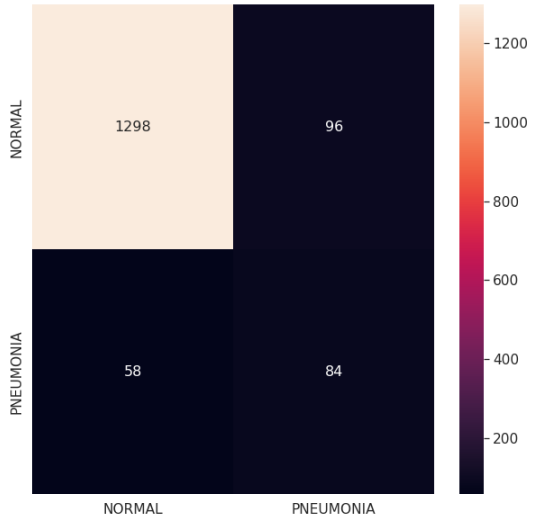

Figure 18: CM after Original ResNeXt101

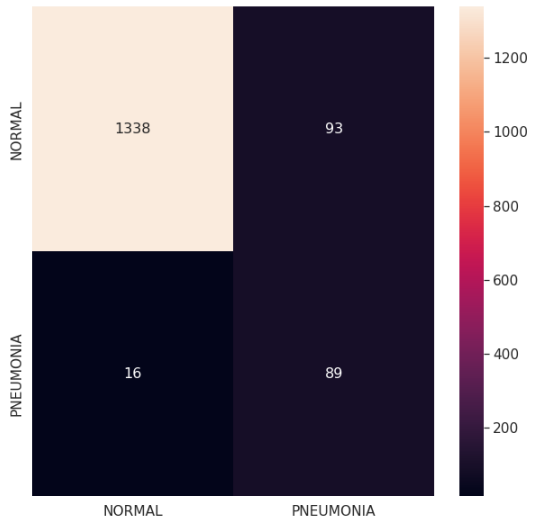

Figure 19: CM after Original DenseNet201

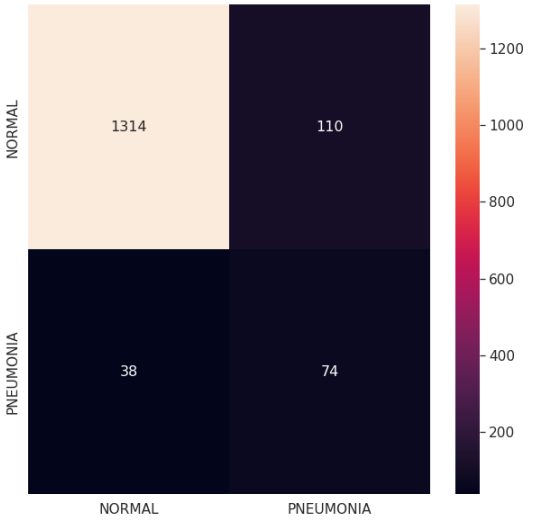

Figure 20.:CM after Original SecrensNet152

V. RESELT OF EXPERIMENT 2: RESULT OF TRNSFER LEARNING

The performances of the six original individual CNN networks SecrensNet152, MobileNetV2, VGG19, ResNet152v2, ResNeXt100 and DenseNet201 are presented in this section. The models' classification performance is first presented. Following that, the overall measures for those models are discussed. gathering, in addition to descriptors, potential causes, and areas for improvement of results.

Table 5. Accuracy for Classification of Individual CNN Networks in Detecting Pneumonia (Transfer Learning CNN Networks)

Architecture	**Training Accuracy**	**Model Accuracy**
VGG19	91.03%	88.11%
ResNet152v2	94.44%	91.98%
MobileNetv2	92.36%	91.47%
ResNeXt101	89.78%	88.19%
DenseNet201	94.44%	92.17%
SecrensNet152	93.05%	91.60%

Six transfer learning CNN architectures' performance is presented in this section. SecrensNet152, MobileNetV2, VGG19, ResNet152v2, ResNeXt101 and DenseNet201 models all had high accuracies in the test sets, as shown in

Table 5. The number of properly-identified samples to the total number of samples was used to compute the test accuracies displayed in Table 5. With a precision of 994.44 %, the ResNet152v2 and DenseNet201 model was the most accurate. The accuracy improvement of the SecrensNet152 network from the initial network to transfer learning is notable.

Table 6. Precision, Recall, F1-Score, and Support (n) result of Transfer Learning CNN networks (based on the number of images, n= numbers)

VGG19				
	Precision	**Recall**	**F1-Score**	**Support**
Normal	0.88	1.0	0.93	1397
Pneumonia	0.0	0	0	187
Accuracy			0.88	
Macro Avg	0.44	0.5	0.46	1584
Weighted Avg	0.77	0.88	0.82	1584
ResNet152v2				
	Precision	**Recall**	**F1-Score**	**Support**
Normal	0.92	0.98	0.95	1397
Pneumonia	0.81	0.41	0.55	187
Accuracy			0.918	
Macro Avg	0.869	0.70	0.75	1584
Weighted Avg	0.91	0.91	0.90	1584
MobileNetv2				
	Precision	**Recall**	**F1-Score**	**Support**
Normal	0.91	0.99	0.95	1397
Pneumonia	0.86	0.33	0.47	187
Accuracy			0.91	
Macro Avg	0.88	0.66	0.71	1584
Weighted Avg	0.91	0.91	0.89	1584
ResNeXt101				
	Precision	**Recall**	**F1-Score**	**Support**
Normal	0.88	1	0.93	1397
Pneumonia	0	0	0	187
Accuracy			0.88	
Macro Avg	0.44	0.5	046	1534
Weighted Avg	0.77	088	0.82	1534
DenseNet201				
Normal	0.92	0.99	0.95	1397
Pneumonia	0.89	0.37	0.53	187
Accuracy			0.92	
Macro Avg	0.91	0.68	0.74	1584
Weighted Avg	0.92	0.92	0.90	1584
SecrensNet152				
	Precision	**Recall**	**F1-Score**	**Support**
Normal	0.92	0.99	0.95	1397
Pneumonia	0.84	0.36	0.50	187
Accuracy			0.91	
Macro Avg	0.87	0.67	0.72	1584
Weighted Avg	0.91	0.91	0.90	1584

The Precision, Recall, F1-score, and Specificity findings from CNN networks incorporating transfer learning are shown in Table 6. In general, a model with high Precision, Recall, and support is a superior model. With a 88%, the trial results show that VGG19 and ResNeXt101 has a low precision in Pneumonia Detection blood cancer.

Training and Validation Accuracy and loss of Transfer Learning CNN Networks:

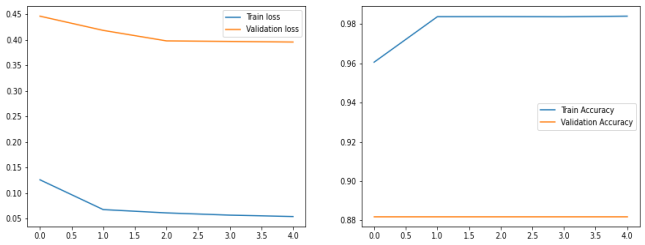

Figure 21: Training and validation accuracy and loss over the epochs (VGG19 Transfer Learning CNN Networks).

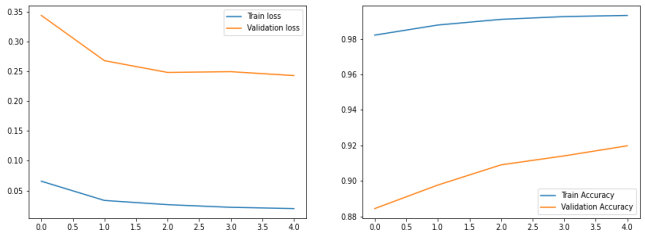

Figure 22. Training and validation accuracy and loss over the epochs (ResNet152v2 Original CNN Networks).

Figure 23: Training and validation accuracy and loss over the epochs (MobileNetv2 Transfer Learning CNN Networks).

Figure 24: Training and validation accuracy and loss over the epochs (ResNeXt101 Transfer Learning CNN Networks).

Figure 25: Training and validation accuracy and loss over the epochs (DenseNet201 Transfer Learning CNN Networks).

Figure 26: Training and validation accuracy and loss over the epochs (SecrensNet152 Transfer Learning CNN Networks).

The training and validation losses of the TL are shown in Figure 26 over epochs. CNN uses a loss function to optimize an architecture. The loss was determined using training and validation data, and the model's overall performance in those sets was used to determine its significance. It is the total number of errors assigned to each instance in each training or validation collection. After each optimization iteration, the loss value represents how well or poorly a model performs.

Confusion Matrix after Transfer Learning (TL) (Based on the number of images:

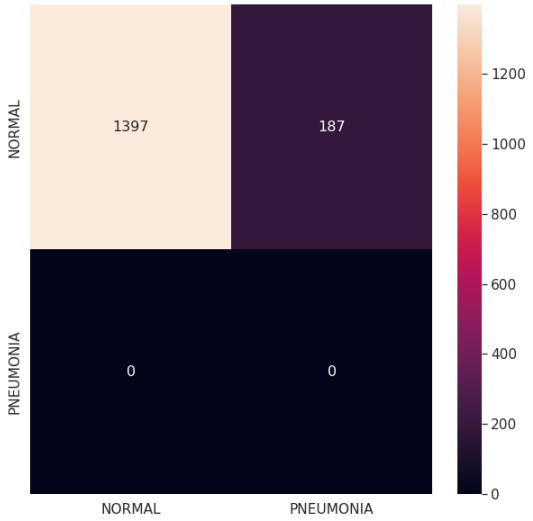

Figure 27: CM after Transfer Learning VGG19

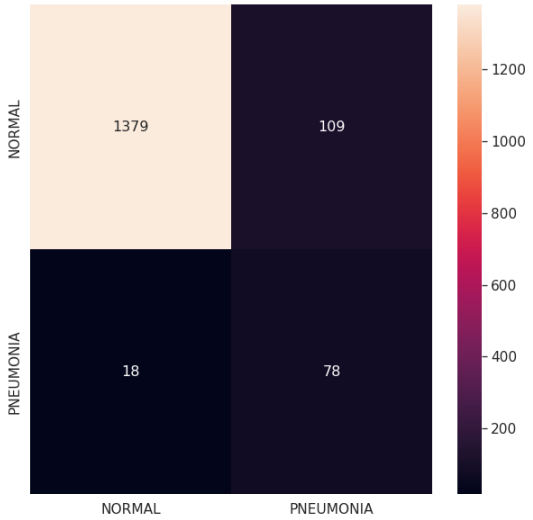

Figure 28. CM after Transfer Learning ResNet152v2

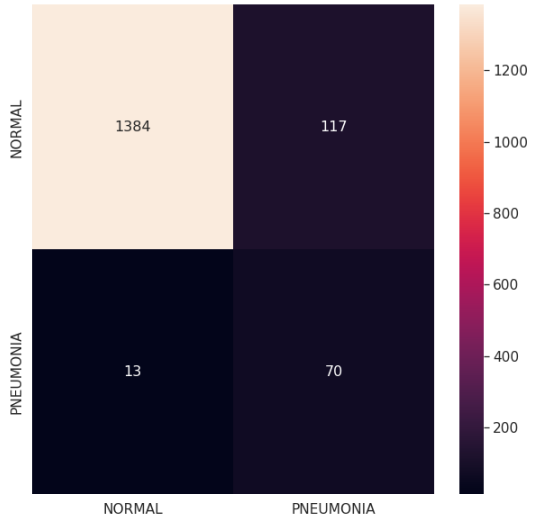

Figure 29: CM after Transfer Learning MobileNetv2

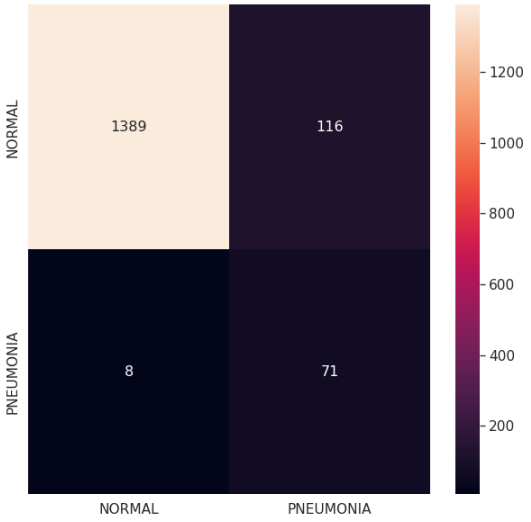

Figure 31: CM after Transfer Learning DenseNet201

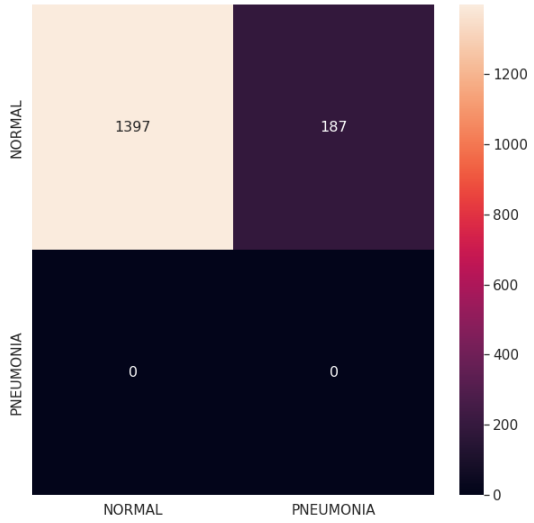

Figure 30. CM after Transfer Learning ResNeXt101

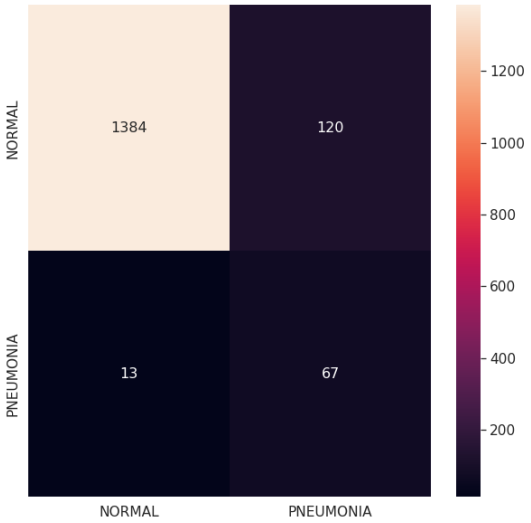

Figure 32: CM after Transfer Learning SecrensNet152

VI. Result of Experiment 3: Ensemble Model Result

Table 7. Ensemble Technique (MXD) CNN Network Accuracy in Detecting Pneumonia

Architecture	**Training Accuracy**	**Model Accuracy**
MXD Model (resnet152v2, seresnet152, mobilenetv2, vgg19, resnext101)	93.15%	93.38%

Table 8. Precision, Recall, F1, and Specificity Result of CNN Networks with Ensemble Techniques (N= Numbers)

Ensamble_MXD_Model (resnet152v2, seresnet152, mobilenetv2, resnext101)				
	Precision	**Recall**	**F1-Score**	**Support**
Normal	0.93	0.99	0.96	3396
Pneumonia	0.92	0.46	0.62	444
Accuracy			0.9338	
Macro Avg	0.92	0.73	0.79	3840
Weighted Avg	0.93	0.93	0.92	3840

The Precision, Recall, F1-score, and Specificity findings from CNN networks incorporating Ensemble Techniques are shown in Table 7. In general, a model with high Precision, Recall, and support is a superior model. With a 93%, the trial results show in Pneumonia.

Training and Validation Accuracy and loss of Ensemble Technique:

Figure 33: Training and validation accuracy and loss over the epochs (Ensemble Technique).

Here from this Figure 31. There showed the validation accuracy is good also loss is not much defective for the model. In a word the new model created is better.

Confusion matrix (CM) after Ensemble Technique (Based on the number of images):

Ensamble_MXD_Model (resnet152v2, seresnet152, resnext101) after considering the images of the datasets. Then after each number of epochs give the confusion matrix of the model, we need to better detection of Pneumonia.

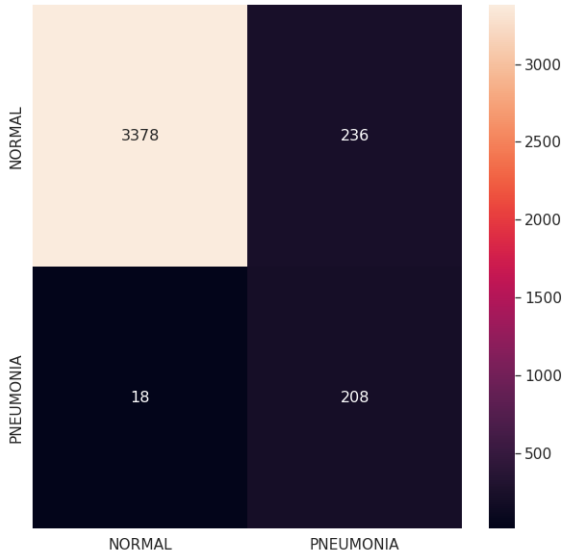

Figure 34: Training and Validation Accuracy and loss of Ensemble Technique

VII. Discussions

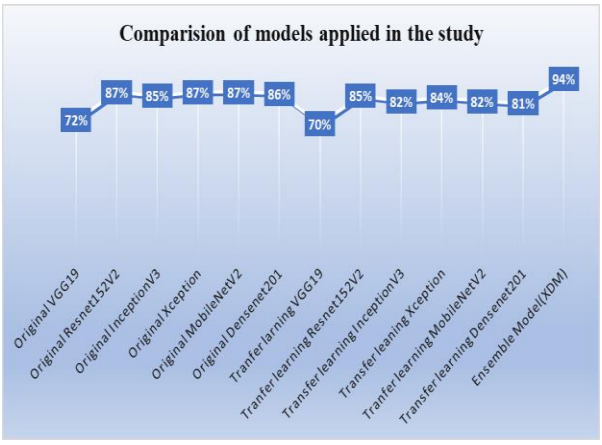

Figure 35: Accuracy comparison among individual CNN, transfer learning and ensemble models

In this research, we performed an in-depth investigation of the performances of the D-CNN in detecting and segmenting four kinds of MRI images of brain tumor (No tumor, Glioma, Meningioma, and pituitary). Results are presented in Figure 33. Total 7022 original images were used in this research. However, image augmentation was carried and eleven image were generated using augmentation from one image.

In the detection study original individual CNN, transfer learning, and ensemble models were used and for detection brain tumor images. For segmenting tumor MR-CNN was used. Though the computation of detection and

segmentation is different, this study aimed of the detection and segmentation computation process.

We compared the results of six different CNN-based models of the SecrensNet152, MobileNetV2, VGG19, ResNet152v2, ResNeXt101 and DenseNet201 by applying them to the two classes of Pneumonia.

Out findings of transfer learning is an agreement with the study that in the case the input image differs from the trained data of Imagenet Dataset, the accuracy is likely to be decreased.The effect of presence of background noise and , the application of different augmentation techniques separately with the test sets resulted in a drop in performance. However, in the case of original CNN, the model was trained and tested using by similar input, the predication capabilities were increased in unseen data. Moreover, although the D- CNN the ability to learn features irrespective of the input data, the limited number of datasets in this study is likely a factor influencing the prediction capability.
Not surprisingly, from our investigation, we found that the ensemble of deep learning models improved its accuracy over a single CNN architecture.

The experiment using MR-CNN for tumor detection and segmentation extracted features by ResNeXt101 and generate RoIs by RPN, preserve the precise spatial position by RoI Align, and generate binary masks through the full convolutional network (FCN). In doing so, the proposed framework is able to detect tumor correctly while also precisely segmenting each tumor in an image. Experimental result suggest that mAp value was 0.95. For the future work, we will consider improving the speed of the proposed method.

VIII. Inference

In this study, deep learning methods are investigated to detect and to segment chest images. The following points in this study can be concluded.

For the same chest image with the same set of data training, the accuracy of classification differs using VGG19, Resnet152V2, MobileNetV2 and DenseNet201. In our study the original Densenet201 and MobileNetV2 achieved highest 94% accuracy.

Though transfer learning aims to improve the performance of a target learner exploiting knowledge in related environments. advocated to use it when source and target datasets have a certain degree of similarity to avoid performance decrease. In our study pin pints that negative transfer which is caused from dissimilar target and source dataset. This outcome stressed the excellence of transfer learning though it has the potential to successfully train deep learning models.

Even if a specific CNN architecture does not perform well, an ensemble of several models still may outperform individual models.

IX. Contributions

A comparison study of chest image classification and segmentation is important to gain a full understanding of CNN performance in brain tumor research using four classes and five thousand images, we presented classification results of original, transfer learning and ensemble learning. Multiple CNN architectures, performance metrics are used for the comparative study, such as inference time, model complexity, computational complexity, and mean per class accuracy. An ensemble model was developed with an aim to increase accuracy and the study confirms that an ensemble model outperforms single CNN architecture. The XDM ensemble model is 75 higher than the accuracy rate of the Resnet152V2, VGG19, SeresNet152, ResNext101 and MobileNetV2. This shows that the XDM ensemble model has a better ability to classify chest image. Thus, the XDM ensemble model has better classification performance and can assist in the diagnosis of Chest image more accurately.

X. Limitations

In this study, a deep learning model was developed to accurately detect and segment two types of construction machineries. The network's performance resulted in an average precision of 0.8792 and inference time of 3173 ms, using a relatively small dataset and a transfer learning technique.

There are a number of limitations in the current stage of the research, which need to address in future work. The use of free-of-charge resources (Google Colab) limits the experiments of this study. As Google Colab offers the server for a limited time, the hyperparameter tuning, training the base model training other than Imagenet (this research used Imagenet as the base database in transfer learning), and the application of Adadelta, FTRL, NAdam, Adadelta, and many more optimizers were not performed in this study. Another limitation is that the research used secondary data that are publicly available, not primary data directly collected from fields.

In the future, we want to create a user interface for the detection and localization of rice leaf diseases for farmers.

This interface would have not only detection but also provide a guide on how the diseases can be controlled. As mobile phones are seen as the preferred technological device among users in developing countries, our aim is to develop a mobile phone-based rice leaf disease detection application tool.

XI. Conclusion and Future Work

Early detection and classification of brain tumor is the topmost necessity to properly diagnose a brain tumor patient. This paper primarily aims to provide a comprehensive performance evaluation of D-CNN on pneumonia detection and segmentation.

Out study suggest that segmentation approach using MR-CNN is effective for small and dirty set of datasets. From our knowledge there is very limited research contributed to specifically to detect pneumonia detection. The comparison study can be highly beneficial for providing better brain tumor management. In the classification of pneumonia, we observed the performance of various CNN models including transfer learning and ensembling. Based on the accuracy, we found that ensemble stack of three network (Resnet152V2, VGG19, SeresNet152, ResNext101 and MobileNetV2) provides better accuracy.

As was previously indicated, however, there were occasions in which the ensemble framework did not come up with accurate forecasts. To that end, we may look into contrast-enhancing or other image-processing approaches in the future. Before classification, we may also use segmentation of the image to help the CNN models get better at pulling out features. Also, because it uses three CNN models for training, the proposed ensemble is more expensive to compute than the CNN baselines that have already been made. In the future, we might use techniques like snapshot ensemble to try to lessen the burden on the computer's resources.

XII. Data Availability

The data of this research are stored in the Kaggle respiratory.

Here the link: Pneumonia_X | Kaggle

References

[1] A. Afifi, N. E. Hafsa, M. A. S. Ali, A. Alhumam, and S. Alsalman, "An ensemble of global and local-attention based convolutional neural networks for COVID-19 diagnosis on chest X-ray images," Symmetry (Basel)., vol. 13, no. 1, 2021, doi: 10.3390/sym13010113.

[2] J. Almirall et al., "Epidemiology of community-acquired pneumonia in adults: A population- based study," Eur. Respir. J., vol. 15, no. 4, 2000, doi: 10.1034/j.1399-3003.2000.15d21.x.

[3] L. R. Baltazar et al., "Artificial intelligence on COVID-19 pneumonia detection using chest xray images," PLoS One, vol. 16, no. 10 October, 2021, doi: 10.1371/journal.pone.0257884.

[4] J. G. Bartlett, R. F. Breiman, L. A. Mandell, and T. M. File, "Community-acquired pneumonia in adults: Guidelines for management," Clinical Infectious Diseases, vol. 26, no. 4. 1998. doi: 10.1086/513953.

[5] J. D. Bodapati and V. N. Rohith, "ChxCapsNet: Deep capsule network with transfer learning for evaluating pneumonia in paediatric chest radiographs," Meas. J. Int. Meas. Confed., vol. 188, 2022, doi: 10.1016/j.measurement.2021.110491.

[6] V. Chouhan et al., "A novel transfer learning based approach for pneumonia detection in chest X-ray images," Appl. Sci., vol. 10, no. 2, 2020, doi: 10.3390/app10020559.

[7] D. K. W. Chu et al., "Molecular Diagnosis of a Novel Coronavirus (2019-nCoV) Causing an Outbreak of Pneumonia," Clin. Chem., vol. 66, no. 4, 2020, doi: 10.1093/clinchem/hvaa029.

[8] E. ERDEM and T. AYDİN, "Detection of Pneumonia with a Novel CNN-based Approach," Sak. Univ. J. Comput. Inf. Sci., 2021, doi: 10.35377/saucis.04.01.787030.

[9] T. Frondelius, I. Atkova, J. Miettunen, J. Rello, and M. M. Jansson, "Diagnostic and prognostic prediction models in ventilator-associated pneumonia: Systematic review and meta-analysis of prediction modelling studies," Journal of Critical Care, vol. 67. 2022. doi: 10.1016/j.jcrc.2021.10.001.

[10] Y. Fujikura et al., "Mortality and severity evaluation by routine pneumonia prediction models among Japanese patients with 2009 pandemic influenza A (H1N1) pneumonia," Respir. Investig., vol. 52, no. 5, 2014, doi: 10.1016/j.resinv.2014.04.003.

[11] Y. Ge et al., "Predicting post-stroke pneumonia using deep neural network approaches," Int. J. Med. Inform., vol. 132, 2019, doi: 10.1016/j.ijmedinf.2019.103986.

[12] E. H. Houssein, Z. Abohashima, M. Elhoseny, and W. M. Mohamed, "Hybrid quantum-classical convolutional neural network model for COVID-19 prediction using chest X-ray images," J. Comput. Des. Eng., vol. 9, no. 2, 2022, doi: 10.1093/jcde/qwac003.

[13] R. Karthik, R. Menaka, and M. Hariharan, "Learning distinctive filters for COVID-19 detection from chest X-ray using shuffled residual CNN," Appl. Soft Comput., vol. 99, 2021, doi: 10.1016/j.asoc.2020.106744.

[14] R. Kundu, R. Das, Z. W. Geem, G. T. Han, and R. Sarkar, "Pneumonia detection in chest X-ray images using an ensemble of deep learning models," PLoS One, vol. 16, no. 9 September, 2021, doi: 10.1371/journal.pone.0256630.

[15] C. C. Kuo, A. M. Gown, E. P. Benditt, and J. Thomas Grayston, "Detection of Chlamydia pneumoniae in aortic lesions of atherosclerosis by immunocytochemical stain," Arterioscler. Thromb. Vasc. Biol., vol. 13, no. 10, 1993, doi: 10.1161/01.ATV.13.10.1501.

[16] T. J. Kuo, C. L. Hsu, P. H. Liao, S. J. Huang, Y. M. Hung, and C. H. Yin, "Nomogram for pneumonia prediction among children and young people with cerebral palsy: A population-based cohort study," PLoS One, vol. 15, no. 7, 2020, doi: 10.1371/journal.pone.0235069.

[17] J. Li et al., "Multi-task contrastive learning for automatic CT and X-ray diagnosis of COVID-19," Pattern

Recognit., vol. 114, 2021, doi: 10.1016/j.patcog.2021.107848.
[18] W. S. Lim et al., “Study of community acquired pneumonia aetiology (SCAPA) in adults admitted to hospital: Implications for management guidelines,” Thorax, vol. 56, no. 4, 2001, doi: 10.1136/thorax.56.4.296.
[19] J. Lu et al., “Identification of antibiotic resistance and virulence-encoding factors in Klebsiella pneumoniae by Raman spectroscopy and deep learning,” Microb. Biotechnol., vol. 15, no. 4, 2022, doi: 10.1111/1751-7915.13960.
[20] T. Mahmud, M. A. Rahman, and S. A. Fattah, “CovXNet: A multi-dilation convolutional neural network for automatic COVID-19 and other pneumonia detection from chest X-ray images with transferable multi-receptive feature optimization,” Comput. Biol. Med., vol. 122, 2020, doi: 10.1016/j.compbiomed.2020.103869.
[21] J. B. Muhlestein et al., “Infection with Chlamydia pneumoniae accelerates the development of atherosclerosis and treatment with azithromycin prevents it in a rabbit model,” Circulation, vol. 97, no. 7, 1998, doi: 10.1161/01.CIR.97.7.633.
[22] N. Nafiiyah and E. Setyati, “Lung X-Ray Image Enhancement to Identify Pneumonia with CNN,” 2021. doi: 10.1109/EIConCIT50028.2021.9431856.
[23] M. Nahiduzzaman et al., “A novel method for multivariant pneumonia classification based on hybrid CNN-PCA based feature extraction using extreme learning machine with CXR images,” IEEE Access, vol. 9, 2021, doi: 10.1109/ACCESS.2021.3123782.
[24] H. Namikawa et al., “Siderophore production as a biomarker for Klebsiella pneumoniae strains that cause sepsis: A pilot study,” J. Formos. Med. Assoc., vol. 121, no. 4, 2022, doi: 10.1016/j.jfma.2021.06.027.
[25] T. Rahman et al., “Transfer learning with deep Convolutional Neural Network (CNN) for pneumonia detection using chest X-ray,” Appl. Sci., vol. 10, no. 9, 2020, doi: 10.3390/app10093233.
[26] S. Ramgopal, L. Ambroggio, D. Lorenz, S. S. Shah, R. M. Ruddy, and T. A. Florin, “A Prediction Model for Pediatric Radiographic Pneumonia,” Pediatrics, vol. 149, no. 1, 2022, doi: 10.1542/peds.2021-051405.
[27] R. P.- Rodriguez et al., “Clinical Performance of The call Score for the Prediction of Admission to ICU and Death in Hospitalized Patients with Covid-19 Pneumonia in a Reference Hospital in Peru,” Pakistan J. Med. Heal. Sci., vol. 16, no. 1, 2022, doi: 10.53350/pjmhs22161474.
[28] N. Y. Saleh, R. A. L. Ibrahem, A. A. hakim Saleh, S. E. shafey Soliman, and A. A. S. Mahmoud, “Surfactant protein D: a predictor for severity of community-acquired pneumonia in children,” Pediatr. Res., vol. 91, no. 3, 2022, doi: 10.1038/s41390-021-01492-9.
[29] M. Shorfuzzaman and M. Masud, “On the detection of covid-19 from chest x-ray images using cnn-based transfer learning,” Comput. Mater. Contin., vol. 64, no. 3, 2020, doi: 10.32604/cmc.2020.011326.
[30] V. S. Suryaa, A. X. Annie R., and M. S. Aiswarya, “Efficient DNN Ensemble for Pneumonia Detection in Chest X-ray Images,” Int. J. Adv. Comput. Sci. Appl., vol. 12, no. 10, 2021, doi: 10.14569/IJACSA.2021.0121084.
[31] A. Ter-Sarkisov, “Detection and segmentation of lesion areas in chest CT scans for the prediction of COVID-19,” Sci. Inf. Technol. Lett., vol. 1, no. 2, 2020, doi: 10.31763/sitech.v1i2.202.
[32] S. F. Tey et al., “Predicting the 14-day hospital readmission of patients with pneumonia using artificial neural networks (Ann),” Int. J. Environ. Res. Public Health, vol. 18, no. 10, 2021, doi: 10.3390/ijerph18105110.
[33] C. C. Tseng et al., “Significance of the modified nutric score for predicting clinical outcomes in patients with severe community-acquired pneumonia,” Nutrients, vol. 14, no. 1, 2022, doi: 10.3390/nu14010198.